analytical chemistry

pubs.acs.org/ac

Article

Understanding and Controlling Spatial Resolution, Sensitivity, and Surface Selectivity in Resonant-Mode Photothermal-Induced Resonance Spectroscopy

Luca Quaroni*

Cite This: *Anal. Chem.* 2020, 92, 3544−3554

Read Online

ACCESS | Metrics & More | Article Recommendations | Supporting Information

ABSTRACT: Photothermal-induced resonance (PTIR) is increasingly used in the measurement of infrared absorption spectra of submicrometer objects. The technique measures IR absorption spectra by relying on the photothermal effect induced by a rapid pulse of light and the excitation of the resonance spectrum of an AFM cantilever in contact with the sample. In this work, we assess the spatial resolution and depth response of PTIR in resonant mode while systematically varying the pulsing parameters of the excitation laser. We show that resolution is always much better than predicted by existing theoretical models. Higher frequency, longer pulse length, and shorter interval between pulses improve resolution, eventually providing values that are comparable to or even better than tip size. Pulsing parameters also affect the intensity of the signal and the surface selectivity in PTIR images, with higher frequencies providing increased surface selectivity. The observations confirm a difference in signal generation between resonant PTIR and other photothermal techniques that we ascribe to nonlinearity in the PTIR signal. In analogy with optical imaging, we show that PTIR takes advantage of such nonlinearity to perform photothermal measurements that are super-resolved when compared to the resolution allowed by the thermal wavelength. Finally, we show that by controlling the pulsing parameters of the laser we can devise high resolution surface sensitive measurements that do not rely on the use of optical enhancement effects.

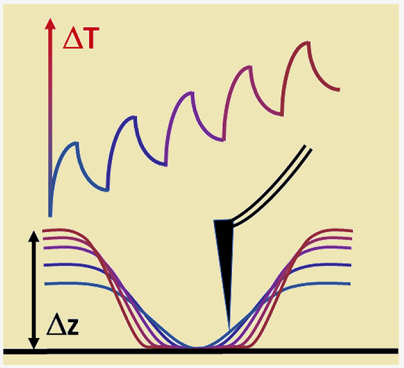

It is well-known that the infrared spectra of a sample provide rich structural and compositional information that is valuable to many areas of research. IR spectroscopy of nanoscale samples is impeded by the modest resolution allowed by diffraction, of the order of a few micrometers. The possibility to achieve spatial resolution beyond the limits imposed by diffraction has driven the development of IR spectroscopy techniques that rely on scanning probe technology. The use of a nanoscale probe placed in contact with, or in the proximity of, the region of interest makes it possible to circumvent the diffraction limit by relying on near-field or proximity effects, including the local amplification of electric fields in the tip−sample contact region and the detection of local sample expansion caused by the photothermal effect.[1] Among IR techniques, photothermal-induced resonance (PTIR) spectroscopy[2] (also referred to as atomic force microscopy infrared, AFM-IR) belongs to a group that relies on the photothermal effect to provide a light absorption spectrum of the sample,[3] including photothermal microspectroscopy (PTMS)[4] and its nanoscale variant scanning thermal infrared microscopy (STIRM),[5] and photoacoustic spectroscopy (PAS), either via acoustic wave detection[6] or via detection of beam deflection.[7] Analysis of the frequency dependence of photothermal excitation provides an IR absorption spectrum of the sample. In PTMS, the local temperature increase is detected by direct contact with a microscopic thermocouple or an element of a Wollaston wire probe, whereas a nanosized resistive AFM probe is used for STIRM. In PAS, a microphone or cantilever is used to measure the acoustic waves generated in an enclosed cell following heat transfer to the gas at the surface of the absorbing sample. Alternatively, deflection of an optical beam can be used to detect the gas density gradient associated with the incipient acoustic wave at the surface of the sample. In AFM-IR/PTIR the deflection or oscillation of an AFM cantilever detects the local sample expansion associated with the photothermal effect in the contact region of the tip. In the present work, the acronym PTIR is used to describe the experiment when implemented with a pulsed light source, to rapidly and simultaneously excite multiple resonances of the AFM cantilever.[8] This choice of terms, although not in universal use, allows us to differentiate the method from other variants of the technique that rely on slow deflection of the cantilever following light modulation at FTIR (acoustic) frequencies.[9]

Received: July 30, 2019
Accepted: February 5, 2020
Published: February 5, 2020

https://dx.doi.org/10.1021/acs.analchem.9b03468
Anal. Chem. 2020, 92, 3544−3554

The resolution of photothermal measurements is generally ascribed to the distribution of thermal waves throughout the sample, which provides resolution values of the order of a few micrometers.[10] The capability of PTIR to achieve a resolution better than allowed by optical diffraction has been ascribed to the use of AFM probes as detectors and justified using different theoretical models.[8,9,11] However, while all existing theoretical models predict resolution better than the diffraction limit, none of them correctly predict the high resolution reported in experimental observations.

The discrepancy between experimental and predicted resolution values highlights the limits in our understanding of the PTIR experiment and in the factors affecting resolution. Part of the difficulty could arise from the interplay of spectroscopic and thermoelastic properties of the sample in generating the PTIR signal, as described in existing theoretical treatments of PTIR intensity.[12] Claims concerning resolution in PTIR are often based on images collected with single wavelength excitation while performing an AFM scan.

An alternative way of assessing PTIR resolution is the use of linear array scans, where PTIR spectra are collected at different discrete locations in space to produce a monodimensional image of the sample from which resolution values are extracted. We call this approach a spectromicroscopy experiment, as opposed to the imaging experiment described in the previous paragraph. While both measurements are sensitive to the mechanics of tip−sample interaction, a spectromicroscopy measurement operates with a stationary tip and avoids any contributions to the image that arise from the movement of the AFM tip, such as from friction and from the settings of the feedback loop. To the best of our knowledge, the relationship between the resolution values obtained in the spectromicroscopy and imaging experiments has not been addressed to date.

In the present work, we aim to clarify the outstanding issues pertaining to resolution in PTIR and compare theoretical models. We provide experimental evidence to understand and support or refute existing claims concerning the spatial resolution of resonant PTIR and we provide the basis for controlling and optimizing spatial resolution, depth profiling, and signal intensity.

EXPERIMENTAL SECTION

All measurements were performed on a nanoIR2 instrument manufactured by Anasys Bruker (Santa Barbara, CA, USA). Excitation was provided by a Daylight Solutions MIRcat quantum cascade laser, with tunable emission in the 1150−1950 cm^{-1} range. The laser beam is delivered to the AFM head by a set of optics that include a polarizer unit. The beam strikes the sample with an incidence angle of size of approximately 70° and is polarized either perpendicular to the sample plane normal (H, horizontal polarization) or 20° to the normal (V, vertical polarization). The laser is focused to a spot approximately 100−200 μm in size and aligned with the AFM tip to optimize the signal. Gold-coated silicon cantilevers (PR-EX-nIR2-10, from Anasys Bruker), with an overall diameter of approximately 100 nm, were used for AFM imaging of the sample and as probes for PTIR spectroscopy and imaging. The tip diameter was measured using a TESCAN Vega3 scanning electron microscope (SEM) operating with a LaB_6 cathode (see Supporting Information section S7).

The experimental sample is a reference provided by Anasys Bruker for instrument testing. It consists of PMMA beads, 3 μm in diameter, embedded in an epoxy matrix and microtomed into thin slices. The sections are supported on a ZnS optical window glued on a metal disk. The section used for this experiment has been measured by its AFM profile to be approximately 150 nm in height.

Spectromicroscopy resolution was estimated by the knife edge method,[13] measuring lines of resonant PTIR spectra across the border between the PMMA bead and the epoxy matrix. A relatively flat region of the PMMA−epoxy contact was chosen for this purpose, to minimize changes of height at the interface, thus reducing or eliminating any interference of topographic structure on the photothermal measurement. The collection of spectra was repeated at different pulse frequencies and duty cycle values of the excitation laser, where the pulse frequency of the QCL laser emission was matched to the modes of the cantilever to satisfy the conditions for resonant mode excitation.[14] The Fast acquisition mode of the instrument was used, corresponding to approximately 20 s for the acquisition of a spectrum in the 1640−1840 cm^{-1} spectral range and approximately 8 min for a single profile of 25 points. The power of the laser was set at 0.1−0.3 mW throughout the spectral range in use. The resolution of each line measurement was assessed by plotting the area of the ester carbonyl absorption band of PMMA around 1730 cm^{-1} as a function of position. For Figure 1A, spectra were collected in 30 nm steps. The distance between the points at 20% and 80% of the edge total height was used as an estimate of resolution. Three measurements for each sample were collected at the same frequency and averaged, to account for the variability introduced by drift, except for 352 kHz, for which only one measurement is available, and 520 kHz, for which two measurements are available. For Figure 1B−D, spectra were collected in 15 nm steps. The full width at half maximum (fwhm) of the first derivative of the profile was used to assess resolution. Three profiles were collected for each experimental condition. Resolution values are reported as the mean of the measurements $\pm$ 1σ.

Pulse duration and pulse interval were calculated from the duty cycle and the pulse frequency assuming a square shape for the pulses.

The same tip is used for all measurements within the same plot, and the same feedback loop parameters are retained throughout all spectra from the same plot. However, different tips were used for experiments shown in different figures, leading to small differences in the resonant frequency values and in measured intensities between different experiments.

The intensity values shown in Figure 2 were obtained by performing repeated measurements in the same location of a PMMA bead section while varying pulse parameters.

PTIR images were collected either by raster scanning the probe at 0.4 Hz with a resolution of 256 points per line in the X and Y directions and averaging 256 pulses, corresponding to a 15.6 nm pixel (Figure 3), or by scanning the probe at 0.2 Hz with a resolution of 64 points per line in the X and Y directions and averaging 128 pulses, corresponding to 62.5 nm pixels (Figure S3). The laser frequency was set at 1730 cm^{-1}, corresponding to a peak absorption of PMMA. PTIR images were not normalized to laser power. Power at the sample was about 0.1−0.3 mW in the spectral region used for this investigation, as for spectromicroscopy measurements.

Measurements satisfy the conditions for resonant mode excitation. The phase locked loop (PLL) algorithm provided by the instrument control software was used during experiments (except those in the Supporting Information Figure S3) to correct for changes in resonance frequency of the cantilever and

https://dx.doi.org/10.1021/acs.analchem.9b03468
Anal. Chem. 2020, 92, 3544−3554

ensure that resonant conditions are maintained despite changes in tip−sample contact. Horizontal profiles of the border between two regions of different composition were extracted from the images of Figure 3 to assess resolution.

RESULTS

Resolution of Resonant PTIR Spectromicroscopy Measurements. We assessed the spatial resolution of resonant mode PTIR by recording a line of spectra across the boundary between two areas of a sample with different composition, PMMA or epoxy, using different values of the pulse frequency, *f*. The resolution of each line measurement is quantified by plotting the area of the ester carbonyl absorption band of PMMA ($\lambda_{max} \sim 5.8\ \mu$m, 1730 cm^{-1}) as a function of position, corresponding to a spectral region where the epoxy matrix does not absorb. We call the resolution of this measurement *Spectromicroscopy Resolution*. While some drift is observed during the measurements, this is accounted for by the standard deviation and appears to provide only a minor contribution to the overall resolution values. The results are plotted in Figure 1A.

Measured resolution under these conditions ranges between 100 and 200 nm and is more than 2 orders of magnitude better than the optical diffraction limit at these wavelengths. The values show a shallow, approximately linear $1/f$ dependence in a log−log plot. In Figure 1A, we also compare this dependence with the one expected if the resolution were limited by thermal wave propagation, as estimated by the parameter *R*.[9] *R* is defined in eq 1 as the radius of a spherical surface at which the amplitude of a thermal wave has decayed to 1/e of its initial value. *R* is called the thermal diffusion limit and is a function of *f*, the modulation frequency of the light, and α, the thermal diffusion coefficient of the material. A typical value of α for an organic polymer is 0.001 cm^2/s.[15,16]

$$R = \sqrt{\frac{3\alpha}{f}} \tag{1}$$

Equation 1 describes the theoretical spatial resolution of PTIR measurements as limited by the diffusion rate of a thermal wave, where *R* is the resolution, *f* is the light modulation frequency, and α is the thermal diffusion coefficient.

Figure 1A shows a plot of *R* versus modulation frequency (red line), revealing a major discrepancy from experimental resolution values. The resolution measured at low frequency is up to an order of magnitude better than the value expected in the thermal diffusion limit. The two plots show a convergent trend at higher frequency values; however, even at the highest frequency, experimental resolution remains at least five times better. In summary, it appears that the thermal diffusion limit does not affect the spatial resolution of resonant PTIR measurements.

To assess the best accessible resolution, we performed systematic measurements by varying both the frequency and duty cycle of the pulsing radiation. While operating at constant power, the pulse duration and interval between pulses vary accordingly and are not independent parameters. Profiles were also collected by using a step size of 15 nm, smaller than nominal tip radius (50 nm). The results are shown in Figure 1B−D. In these measurements, we used the fwhm of the profile as a measure of resolution, different from what was used in Figure 1A. The use of the fwhm of the profile provides lower resolution values than the use of the 20%−80% distance (about 30%−40% lower) and provides a closer match to the resolution values estimated by the Rayleigh criterion.[13] However, it is also more sensitive to noise and only some resonances provide a useful signal-to-noise ratio. As expected, the measurements in Figure 1B−D show both lower resolution values and greater variance. Nonetheless, they confirm the weak dependence of resolution on pulse frequency reported in Figure 1A. They also show that

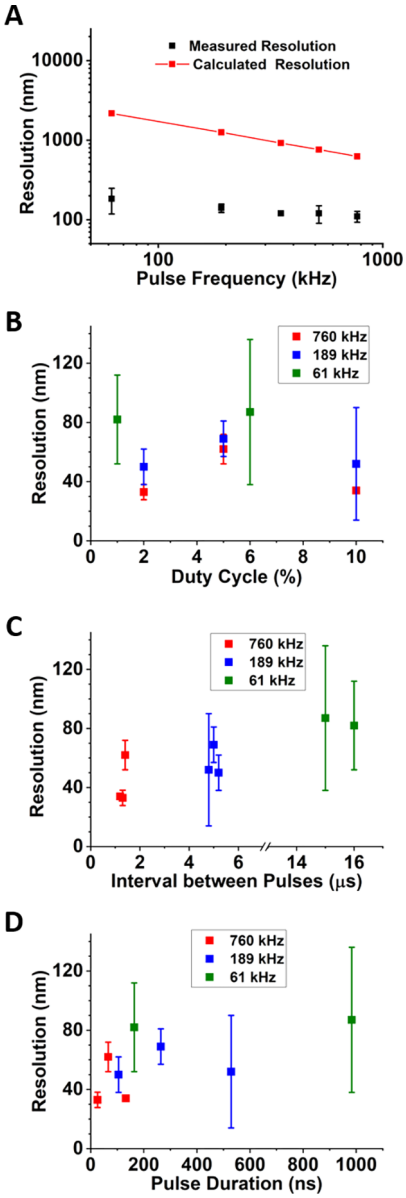

Figure 1. Dependence of spatial resolution in spectromicroscopy line scans on the laser pulse structure. All points were recorded using a QCL laser pulsed at the same frequency as a cantilever resonance. Experimental measurements are reported as mean ± 1σ. (A) Comparison between measured resolution as a function of frequency at constant duty cycle (20%−80% edge distance on profiles measured with 30 nm steps, 4% duty cycle) and expected resolution based on the calculated values of the thermal diffusion limit. (B) Limiting resolution measured as a function of duty cycle and frequency (fwhm of the derivative of profiles measured with 15 nm steps). (C) Limiting resolution measured as a function of pulse duration and frequency (fwhm of the derivative of profiles measured with 15 nm steps). (D) Limiting resolution measured as a function of pulse interval and frequency (fwhm of the derivative of profiles measured with 15 nm steps).

https://dx.doi.org/10.1021/acs.analchem.9b03468
Anal. Chem. 2020, 92, 3544−3554

the best resolution values are provided by higher frequency, shorter pulses, and longer intervals between pulses. The best achieved resolution is approximately 30 nm, smaller than the diameter of the tip used in these experiments. As a general trend, resolution values measured at higher frequency show lower variance. This appears to be due to reduced levels of noise in higher frequency measurements and is consistent with the $1/f$ frequency dependence of electronic noise in the system and the use of lock-in amplifiers to recover the signal at the various resonances.

Signal Intensity and Depth Response of PTIR Spectromicroscopy Measurements. Most photothermal measurements show a dependence of signal intensity on the modulation frequency of the light source because of their dependence on thermal wave propagation, as in the case of PAS.[6] To probe the existence of any such dependence in PTIR experiments, we have measured the relationship between signal intensity and pulse frequency of the laser in one location, approximately in the middle of a PMMA bead section. Measurements were performed with the V polarization at constant power while varying the frequency and duty cycle of the laser. Pulse length and time between pulses are automatically changed as dependent parameters, allowing us to investigate the dependence of the signal from the overall pulse structure, not only the frequency.

Figure 2A shows the relationship between the signal intensity, duty cycle, and frequency of the pulses at constant power. At all frequencies, the intensity increases with duty cycle following approximately linear trends, with different frequencies displaying different slopes. The difference in slope is presumably dominated by the Q factor of the individual resonances from which the PTIR signal is expected to depend linearly. Parts B and C of Figure 2 plot the same measurements as a function of the corresponding values of pulse duration and interval between pulses. Extending the pulse duration and decreasing the interval between pulses both provide increased intensity. The observed dependence of signal intensity from pulse structure shows that individual pulses do not behave independently in shaping the overall PTIR signal. This has been confirmed by measuring signal intensity while averaging an increasing number of pulses and is shown in Figure 2D for two different values of frequency and pulse length. The averaging of independent pulses is expected to lead to an improvement in signal-to-noise ratio at constant signal. A decrease in variance with the number of pulses shows that signal-to-noise levels do indeed improve with averaging, as expected. However, signal intensity also changes. At a lower frequency (64 kHz, 6% duty cycle, 938 ns pulse length, 15 μs interval) the change is irregular. However, at a higher frequency (520 kHz, 6% duty cycle, 115 ns pulse length, 1.8 μs interval) the signal increases monotonically until it reaches apparent saturation.

Resolution and Depth Response of Resonant PTIR Imaging Measurements. To evaluate spatial resolution in the imaging configuration, we recorded PTIR images of the sample using excitation in the ester carbonyl band of PMMA. The laser was pulsed in resonance with one harmonic of the cantilever, while performing an AFM scan in contact mode. In this work, the resolution extracted from profiles in PTIR images is called *Imaging Resolution*. Measurements were repeated at different values of the duty cycle to assess the effect of pulse length and pulse separation. All of the measurements were performed with V polarization. We extracted profiles of the border between PMMA and epoxy at different locations and used the width of

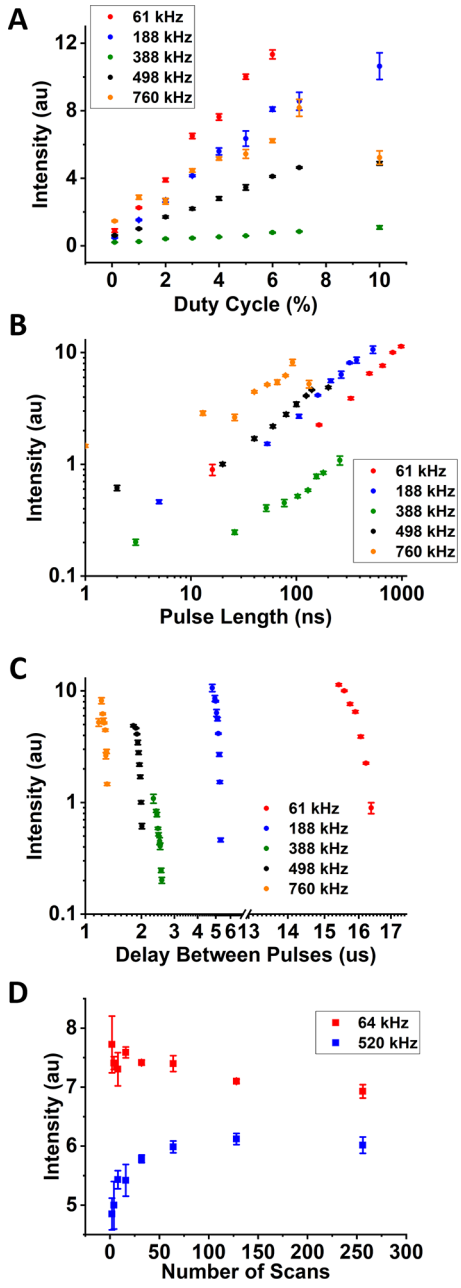

Figure 2. Dependence of signal intensity in spectromicroscopy PTIR experiments on the pulsing parameters of the laser at constant power. Intensity values correspond to the area of the PMMA absorption peak at 1730 cm^{-1}. Measurements are reported as mean $\pm$ 1σ. (A) Intensity measured as a function of duty cycle and frequency. (B) Intensity measured as a function of duty pulse length and frequency. (C) Intensity measured as a function of delay between pulses and frequency. (D) Intensity measured as a function of the number of scans averaged in a measurement.

the edge scan at the points where height is 10% and 90% of maximum as an estimate of resolution. During the same scan we recorded height, deflection, and lateral deflection images for comparison. PTIR images are shown in Figure 3, while the resulting resolution values are shown in Figure 4.

The images in Figure 3 show an unexpected trend, in which PTIR image quality and the amount of discernible detail increase with pulsing frequency and duty cycle. Therefore, the trend in image quality follows the trend from the single point spectral

https://dx.doi.org/10.1021/acs.analchem.9b03468
Anal. Chem. 2020, 92, 3544−3554

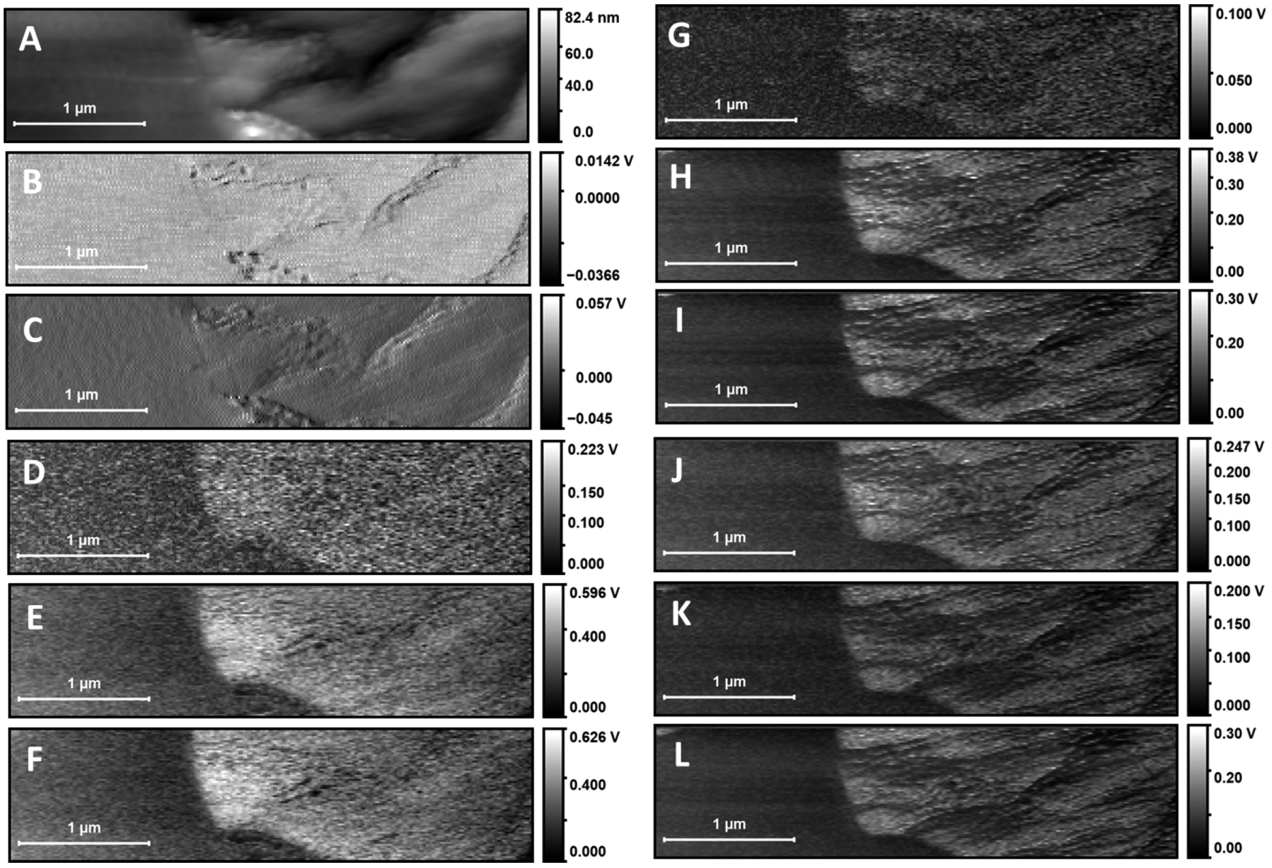

Figure 3. Dependence of PTIR images of PMMA bead sections from pulse structure. All images recorded with V polarization. Retrace only is shown. (A) AFM height. (B) AFM lateral deflection. (C) AFM deflection. (D) 61 kHz, 1% duty cycle. (E) 61 kHz, 5% duty cycle. (F) 61 kHz, 10% duty cycle. (G) 189 kHz, 1% duty cycle. (H) 189 kHz, 5% duty cycle. (I) 189 kHz, 10% duty cycle. (J) 760 kHz, 2% duty cycle. (K) 760 kHz, 5% duty cycle. (L) 760 kHz, 10% duty cycle.

measurements reported in Figure 2. However, Figure 3 also shows qualitative changes in image appearance occurring as a function of frequency. The lower frequency images, at 61 kHz, show little detail. In contrast, images at a higher frequency show a wealth of detail on the nanometer scale, more than is observed in the height, deflection, and lateral deflection images. This is particularly true for the images collected at 760 kHz, where features as close as 30 nm can be resolved, comparable to and smaller than the tip diameter. Increasing duty cycle appears to improve image quality without adding new detail.

In assessing the role of thermal wave distribution in PTIR signal generation, it is useful to compare the results in Figure 3 with the thermal diffusion length, L,[17] defined by eq 2. L represents the distance from the surface of the absorbing volume at which the amplitude of a thermal wave generated at the surface has decayed to 1/e of its initial value.[6] This quantity can be used to express the depth probed by a photothermal measurement and is related to R by a factor of ∼3.

$$L = \sqrt{\frac{\alpha}{\pi f}} \tag{2}$$

Equation 2 describes the thermal diffusion length of a thermal wave from the surface of an absorbing region. L is the thermal diffusion length, f is the light modulation frequency and α is the thermal diffusion coefficient. For a polymer, α is of the order of 0.001 cm^2/s.

Equation 2 defines the capability for depth profiling of measurements that rely on the photothermal effect and is often used in PAS measurements[18] and in measurements that rely on thermal wave propagation in general.[19] At the lowest pulsing frequency used in Figure 3, 61 kHz, L is approximately 2 μm, far larger than the thickness of the PMMA layer. It decreases to about 400 nm at 189 kHz and to 200 nm at 760 kHz, becoming comparable to the thickness of the layer. Therefore, the thermal wave expands through the full sample thickness at all frequencies used in these experiments, although at higher frequencies it is more localized to the proximity of the upper sample surface. This case is intermediate between those of thermally thick and thermally thin samples, as defined by Rosencwaig et al.[6] The sharp changes in image structure observed with increasing frequency suggest that the surface sensitivity and selectivity of the PTIR experiment is greater than predicted from the thermal diffusion length L. The same conclusions are reached when measuring with different polarization of the incident light (Supporting Information Figure S3).

Figure 4 shows that imaging resolution from edge scans is much better than expected according to R, as described by eq 1 and plotted in Figure 1A, and slightly worse than but comparable to spectromicroscopy resolution. It is also affected by the direction of tip movement relative to the boundary. As in the case of spectromicroscopy experiments, the resolution shows a shallow dependence on the pulsing frequency, with higher frequency, shorter pulse length, and shorter interval between pulses providing better resolution. Resolution was measured for both the trace and retrace profiles, and the two measurements are reported separately in Figure 4. Interestingly the resolution

https://dx.doi.org/10.1021/acs.analchem.9b03468
Anal. Chem. 2020, 92, 3544−3554

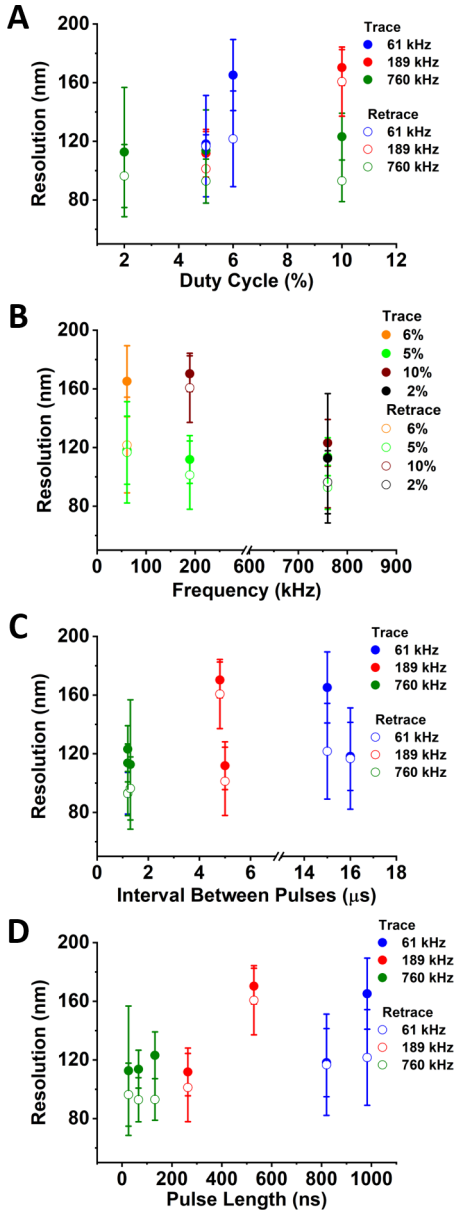

Figure 4. Resolution in PTIR images. Resolution values have been extracted from profiles in the PTIR images in Figure 3 (10%−90% edge distance with 15 nm pixel size). Measurements are reported as mean ± 1σ. (A) Resolution as a function of duty cycle, frequency, and scan direction. (B) Resolution as a function of frequency, duty cycle, and scan direction. (C) Resolution as a function of pulse interval, frequency, and scan direction. (D) Resolution as a function of pulse length, frequency, and scan direction. In the trace scan, the tip moves away from the absorbing region. In the retrace scan, the tip moves toward the absorbing region.

values obtained while scanning in the two directions are slightly but appreciably different. Resolution is better when the tip is moving in the retrace scan, from the epoxy toward the PMMA absorber. Measurements were performed under conditions that matched within 30 nm the AFM height profile in the trace and retrace directions. A small mismatch is also observed between the PTIR trace and retrace images, which disappears only at the slowest scan rates.

DISCUSSION

PTIR Spectromicroscopy Resolution and Thermal Wave Propagation. In spatially resolved photothermal experiments, limiting spatial resolution is generally attributed to the propagation of the thermal wavefront created by light absorption. In the case of excitation by a single impulse of light, the temperature front expands away from the absorption region at a rate determined by the thermal diffusion coefficient of the material while decaying in intensity. The extension of the thermal wavefront is called the thermal diffusion limit. When excitation is extended to a series of pulses, a train of waves is formed. The resulting temperature variation in the sample oscillates at the same frequency as the source of excitation and is termed a thermal wave. A thermal wave decays in space at a rate that is a function of its frequency. Higher frequencies correspond to a more rapid decay in space and limit the size of the expansion zone, allowing higher spatial resolution. By analogy with optical imaging and spectromicroscopy, the model describes resolution as limited by the wavelength associated with the thermal wave, called the thermal wavelength (see the Supporting Information).[10] Thermal wavelengths vary over several orders of magnitude, depending on modulation frequency and the thermal properties of the sample. The quantities R and L, also related to this model, predict resolution values of the order of several hundred nanometers for the experimental conditions commonly used in PTIR and AFM-IR experiments, better than those allowed by diffraction but poorer than those reported in the literature and measured in our experiments, as shown in Figure 1. This model has been used to describe the resolution of scanning probe photothermal measurements[17] and as a reference parameter for limiting resolution in AFM-IR experiments with synchrotron light.[9]

The first theoretical treatment that specifically addresses resolution in PTIR was developed by Dazzi in the same work that coined the PTIR acronym.[8] It was the first effort to analyze spatial resolution as a function of sample mechanical parameters and measurement conditions specific to PTIR. The treatment entails two limiting cases that are relevant for the general interpretation of PTIR experiments. In one case, the absorbing object is located on top of a nonabsorbing substrate, leading to a lateral spatial resolution that is limited by tip size. In the second case, the absorber is embedded in a nonabsorbing matrix made from a soft material. In the latter case, the matrix expands with the object and resolution is limited by the extension of the expansion zone, as determined by the properties of the absorber. This model correctly predicts that PTIR resolution can reach values well below the diffraction limit for absorbing objects that are themselves much smaller than the imaging wavelength. However, as the size of the object becomes comparable to the wavelength, it provides resolution values that are closer to the ones obtained in optical far field measurements. The application of the model to our case leads to a calculated spatial resolution of the order of approximately 2.3 μm (see the Supporting Information Section S2), comparable to that calculated for the lowest frequency resonance in the thermal diffusion limit (Figure 1) but larger than the value we measured experimentally.

An expanded theoretical treatment by Morozovska et al.[11] includes features of both models described previously and addresses the interplay between thermal diffusion and the thermoelastic properties of both absorber and embedding matrix on the geometry of photothermal expansion. The model reveals a dependence of the modulation frequency on resolution, with a

https://dx.doi.org/10.1021/acs.analchem.9b03468
Anal. Chem. 2020, 92, 3544−3554

higher frequency leading to improved resolution. It provides calculated resolution values that are better than diffraction limited resolution but also poorer than values reported for impulsive PTIR and values measured in our experiments (Figures 1 and 4). To date this treatment has been restricted to slow sinusoidal excitation, as used in PTMS, and has not been extended to the impulsive excitation used in PTIR.

The experimental results presented in the previous section allow us to systematically compare existing theoretical models of PTIR resolution. Figure 5 schematically sums up the problem.

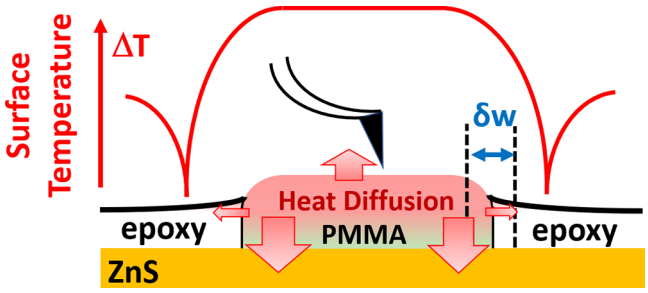

Figure 5. Graphical representation of proposed thermomechanical changes in the sample following light absorption. The PMMA region absorbs modulated light and its temperature increases, leading to expansion. Modulation of the light source generates a thermal wave that propagates and decays away from the absorbing region. The substrate, epoxy matrix, atmosphere and tip all act as thermal sinks, leading to a gradient of temperature between the surface and the substrate. The surface temperature increase associated with the thermal wave is shown qualitatively as a graphical representation based on calculations from ref 20 and is not drawn to scale. Only the expansion of the absorbing PMMA region causes excitation of cantilever resonances in its proximity. The propagating thermal wave is not detected by PTIR, despite the local temperature increase. The limit to resolution is given by the distance, δw, at which the expansion of the edge of the PMMA region is detected.

Light absorption by PMMA causes a localized temperature increase and expansion of the absorbing region. Because of the periodical structure of the excitation, the temperature increase distributes through the sample in accordance with the properties of thermal waves and can lead to expansion of the sample beyond the absorption region, such as in the epoxy region in contact with PMMA. The temperature perturbation decays in space and time following heat transfer to several heat sinks, including substrate, epoxy matrix, tip, and air. Sample expansion is detected via excitation of the mechanical resonances of an AFM cantilever. The spatial resolution of the PTIR measurement depends on the capability to measure and resolve the edge of the expansion region, represented by δw in Figure 5.

To test the existing models of PTIR resolution, we resort to resonant excitation. Pulsed excitation presents several differences from smooth sinusoidal excitation, particularly for what concerns the rapidity of the resulting temperature variation. This is described by a rapid exponential increase in temperature, determined by pulse duration, and is followed by an exponential relaxation.[21] Despite these differences, a train of light pulses (and the resulting raise and decay temperature profiles in the sample) can be generally described as the Fourier synthesis of a sinusoidal fundamental and its odd harmonics, where the fundamental oscillates at the pulsing frequency. As the fundamental provides the dominant contribution, its frequency can be used as an estimate of the extension of the thermal wave generated by absorption. This approach allows us to compare measured spatial resolution to the propagation characteristics of thermal waves generated in a PTIR experiment, as determined by the thermal diffusion coefficient and the pulsing frequency of the source (eq 1[9] or eq 2[17]). As in the case of simple sinusoidal excitation, increasing the pulsing frequency is expected to reduce the spatial extent of the wave and improve resolution. While this trend is observed in our experiments, the measurements presented in Figure 1 also show that experimental resolution in spectromicroscopy is about 1 order of magnitude better than R, indicating that thermal wave propagation is not a limiting factor. A discrepancy from calculated values of R was also reported by Donaldson et al.[9] when testing the resolution of an AFM-IR instrument on a synchrotron beamline.

An additional relevant observation comes from the interesting work of Chae et al.,[22] who used sensitive optomechanical transducers to measure the time evolution of the PTIR response in a sample similar to the one used in the present work. These authors followed the PTIR signal for several microseconds after excitation while positioned on a PMMA bead section. While they observed the response of the tip due to excitation of the contact region, their data do not show the propagation of the thermal front from nearby absorbing beads, which is expected to arrive after 100 μs (based on the thermal diffusion rate of the sample, of the order of 0.001 cm^2/s). Their PTIR images show that PMMA beads are well resolved, as in our experiments, confirming that thermal wave propagation does not limit resolution in their experiment.

Despite the lack of a correspondence with either R or L, measured resolution displays a dependence on $1/f$ in a log−log plot, as observed for other signals that depend on the photothermal effect, such as the photoacoustic signal.[6] The observation of this dependence also shows that tip size does not limit resolution for most of the frequency range explored in this work. However, resolution of approximately 30 nm, smaller than tip radius, can be achieved when using the highest frequency resonance and the highest duty cycle available from this setup, 760 kHz (approximately, depending on tip resonance) and 10%, respectively, as shown in Figure 1B. It is often stated or implied in the literature on the subject that PTIR allows the measurement of IR absorption with AFM resolution. We now show that this is not generally true, but it can be achieved under specific conditions. We must stress that the limiting resolution values reported in this work are set by the frequency and duty cycle accessible to the instrument. We do not presently know if resolution much smaller than tip size can be achieved and what the fundamental limits, set by the physics of the experiment, are.

Imaging Mode Resolution. Similarly to the case of spectromicroscopy, spatial resolution in imaging mode appears to be much better than allowed by the thermal diffusion limit and worse than allowed by tip size. However, it is also different from, and somewhat worse than, resolution in spectromicroscopy mode. It is also notable that small differences in resolution are observed when scanning away from or toward the absorbing region (Figure 4). Interestingly, while resolution smaller than tip radius can be achieved when measuring with a stationary tip, using high frequency and high duty cycle, resolution comparable to tip diameter is achieved in imaging mode (Figure 4). The difference cannot be explained in terms of pixel size, which is 15 nm in the images of Figure 3, similar to the step size used in spectromicroscopy experiments. Variations in sample thermoelastic parameters could give rise to differences in resolution, by affecting image contrast.[11] However, the bulk mechanical and thermal properties of PMMA and epoxy in our sample are

https://dx.doi.org/10.1021/acs.analchem.9b03468
Anal. Chem. 2020, 92, 3544−3554

similar or identical[11] and their variation is expected to provide a small or negligible contribution to the contrast observed in the images of Figure 3. Furthermore, according to current theory, the amplitude of the PTIR signal is expected to be affected in the same way whether the tip is stationary or it is scanned.[12] Therefore, the differences reported for spectromicroscopy and imaging experiments cannot be explained simply in terms of differences in mechanical properties within the sample. It is not clear from the present measurements if the difference has a physical or an instrumental origin, i.e., if it is due to the specific features of PTIR signal generation or to the way the signal is processed by the instrument or both.

It is noteworthy that, despite the homogeneous bulk properties of the sample, the PTIR images in Figure 3 show fine patterns that cannot be explained by differences in sample composition or in sample thickness. PMMA regions have PTIR intensity changing over the full scale, despite the nominally homogeneous composition. Inside the beads, the PTIR signal is close to zero in some locations, while it is maximal in other locations. The variability cannot be fully explained by the irregularity of the sections, despite local thickness variations of tens of nanometers. Therefore, the PTIR intensity in the images does not linearly track the composition of the sample. The higher frequency PTIR images in Figure 3 show a remarkable number of fine details, which are not seen in any of the mechanical AFM images, including ridges and crests running in roughly parallel patterns. Not even lateral deflection images, particularly sensitive to the friction of the surface, show such detail. Patterns 30 nm apart can be appreciated, indicating an apparent resolution even smaller than tip radius and better than the resolution values extracted from edge profiles on the same image. We do not know what these structures are, but they are reproducible in all images at a higher frequency, indicating that they are not simple instrumental artifacts. Their contrast could arise from the interplay of surface structure with the movement of the scanning AFM probe, resulting in changes in tip−sample contact, whereby deflection and torsion of the cantilever are affected by friction and adhesion. However, variations in mechanical properties would likely also be appreciated in AFM measurements, such as those of lateral deflection, and this is not seen in the corresponding maps of Figure 3. An additional possibility is given by local variations in thermal properties that affect heat dissipation toward the tip, and it will be addressed in the next section of the discussion. Other unidentified interactions between the tip and the PMMA sample may also play a role. Further investigation is necessary to clarify the origin of the contrast observed in Figure 3. Nevertheless, Figure 3 clearly highlights the existence of subtle differences between the PTIR response in spectromicroscopy and imaging experiments. The newly developed tapping AFM-IR configuration may provide information in this respect by providing images that remove the dependence of the signal on the Young modulus of the sample, although it retains a dependence from a nonlinear elasticity factor.[23]

Comparison with Theoretical Models. All existing models of resolution in PTIR and AFM-IR experiments fail to predict the resolution values observed in our experiments. To interpret this conclusion, it is useful to compare PTIR results to the direct measurement of temperature increase in the sample. Katzenmeyer et al. used STIRM to image the photothermal-induced temperature increase in a section of PMMA beads embedded in epoxy.[5] While the authors do not consider this interpretation, their images do provide a temperature line profile consistent with the calculated distribution of a thermal wave in a supported thin film.[20] Their STIRM images of PMMA have relatively low resolution, as expected from the spatial distribution of thermal waves (see the Supporting Information for a detailed comparison), while the PTIR images of the same sample show better resolution.

The observations of Katzenmeyer et al. confirm our conclusion that the PTIR signal does not respond linearly to the temperature increase associated with thermal wave distribution. A discrepancy between the experimental PTIR signal intensity and calculated sample expansion under impulsive excitation has already been noted by Dazzi.[24] The calculated expansion of a sample of 150 nm thickness, as in our case, is of the order of tens of picometers.[11] A tip displacement of this order of magnitude should be undetectable under the conditions of our measurement without the use of higher excitation power. Nonetheless a strong PTIR signal is obtained. This discrepancy led to the early suggestion by Dazzi et al. that the rapidity of the expansion when using impulsive excitation could contribute to the intensity of the PTIR spectrum,[24] raising the possibility that the mechanism of signal generation may be different when using impulsive and nonimpulsive excitation. This concern has also been expressed by Morozovska et al.[11], who stress that the results of their calculations can model resolution in PTMS or PTIR with nonimpulsive excitation but not the case of PTIR with rapid impulsive excitation, as used in our experiments. In agreement with these authors, we propose that the difference between values of spatial resolution measured in our experiments and theoretical values could be due to the different time structures of the exciting light.

Signal Intensity, Depth Response, and Pulse Structure in Resonant PTIR. To understand the discrepancy between observed and theoretical resolution and between temperature increase in the sample and signal intensity, we have analyzed the effect of pulse structure on signal intensity. The issue has received little attention to date. The theoretical treatment by Dazzi et al.[24] considered two different regimes, using either pulses from an OPO laser, shorter than the relaxation time of the sample, or pulses from a free electron laser, longer than the relaxation time. Experiments using two different lasers with different pulse duration have also been carried out by Katzenmeyer et al.[25] In neither case did the authors address the role of pulse length on resolution.

Figure 2 reveals a strong dependence of signal intensity on the structure of the excitation pulses. Increasing the duty cycle of the laser from 0.1% to 10% while keeping power constant can change signal intensity by more than 1 order of magnitude, depending on the specific resonance. Intensity increases steeply when decreasing the interval between pulses; a decrease in pulse spacing of less than 10% can lead to an increase in intensity of 1 order of magnitude. The observations indicate that the sample does not fully relax between pulses, i.e., the response to a pulse train is not the average of the response to the individual pulses. This is most obvious in Figure 2D, showing that the averaging of scans monotonically improves signal intensity at short pulse interval and high frequency. The increase in intensity with scan number is not observed when measuring at the lowest accessible frequency, corresponding to a large pulse separation, greater than 15 μs, suggesting that nearly complete relaxation of the system is achieved at such long intervals. To our knowledge, this behavior has not been reported to date and can provide a means to interpret several aspects of PTIR experiments.

https://dx.doi.org/10.1021/acs.analchem.9b03468
Anal. Chem. 2020, 92, 3544−3554

The relationship between signal intensity and pulse structure can be understood by considering that repeated excitation of the sample in the absence of complete relaxation can generate a nonlinear photothermal response if the response of the system changes with temperature. This is schematically represented inFigure 6.

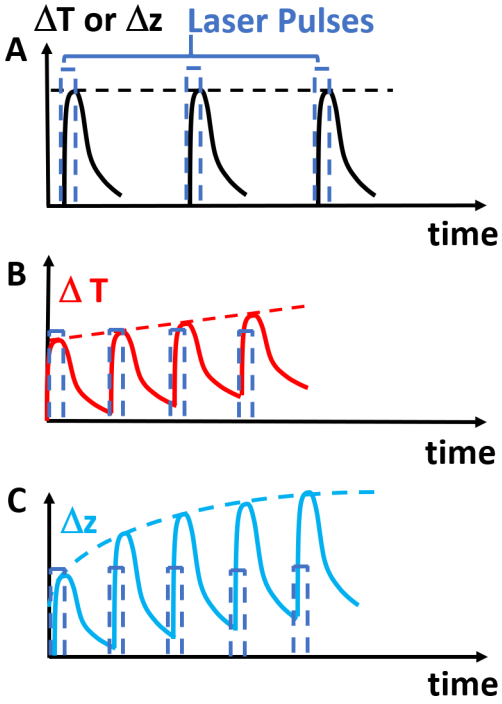

Figure 6. Change in photothermal response as a function of pulse structure. (A) In the case of nonoverlapping pulses, where the system can fully relax (thermalize) between pulses, the temperature evolution of the sample, ΔT, and the expansion from the sample, Δz, are identical after each pulse. (B) In the case of overlapping pulses, the sample cannot thermalize between pulses and the temperature T increases progressively as the effect of multiple pulses builds up. (C) If the response of the system changes with temperature and the sample is not allowed to thermalize, then the addition of successive pulses leads to a temperature buildup and increased nonlinear sample expansion Δz.

In the simplest model, a nonlinear response can be accounted for by the temperature dependence of the Grüneisen parameter Γ (see the Supporting Information). For many soft materials, Γ shows an increase with temperature, resulting in larger expansion at higher temperature. In a pulsed photothermal experiment, the temperature dependence of Γ results in increased expansion with successive pulses if the system is not allowed to thermalize between pulses. Each new pulse excites the system to a progressively higher temperature and generates larger expansion (Figure 6). The temperature dependence of Γ is used in Grüneisen relaxation photoacoustic microscopy (GR-PAM) to achieve spatial resolution better than allowed by optical diffraction at infrared wavelengths.[26] While our experimental scheme is different from the one used for GR-PAM, the temperature dependence of Γ can be used to explain and control the spatial resolution of any experiments that rely on photothermal expansion. In the presence of a temperature gradient, photothermal excitation by a pulse of light induces larger expansion at the higher temperature extreme of the gradient, provided that Γ increases with temperature. This is amplified as the number of pulses builds up if the sample does not fully relax between pulses. The resulting photothermal response is nonlinear with temperature and is shaped by the pulsing parameters of the laser, including frequency and duty cycle. The eventual determinant of spatial resolution is expected to be the interplay between the pulse parameters of the laser and the thermal conductivity of absorber and surroundings, which act as a heat sink. This observation suggests that the use of thinner samples may lead to improved resolution because of changes in thermal contact between the absorbing region and the support.

While our results can be qualitatively explained by the nonlinearity of thermal expansion, the studies by Chae et al.[22] suggest that the situation may be more complex and that heating of the interfacial gas layer may be an important factor in determining the overall nonlinearity of the PTIR response, highlighting a potential similarity between the mechanism of PTIR signal generation and the mechanism of PAS signal generation.

The increase in PTIR resolution allowed by the nonlinear response of the sample is analogous to the gain in resolution that is obtained in optical imaging via a nonlinear optical response.[26] In the case of resonant PTIR, one can overcome the resolution limit set by the thermal wavelength, of the order of micrometers, by achieving a lower limit set by the interplay of the photothermal expansion zone and tip−sample interactions, of the order of tens of nanometers.

Cases of nonlinearity in the PTIR response have also been reported in experiments with nonresonant excitation, concerning different aspects of the measurement, including the observation of unusually sharp bands,[27] giving higher spectral resolution than the corresponding FTIR spectra,[28] and in the differential response from cellular regions.[29] It is presently unclear if effects observed under nonresonant conditions are related to the nonlinearity discussed in the present work.

Role of Optical Enhancement on Resolution. It should be pointed out that the case of tip-enhanced resonant PTIR of monomolecular layers on a nonabsorbing substrate, such as in the original reports of tip-enhanced resonant PTIR by Lu et al.,[30] warrants different considerations in assessing resolution, as already pointed out by Dazzi.[8] In addition, the use of an optical configuration for tip enhancement optics (a sharp gold tip and a gold support separated by a few nanometers) and high incident power (3 orders of magnitude higher than in the present work) is expected to provide measurable vertical expansion from the upper surface of the sample but negligible expansion in the perpendicular direction, at the edges of the absorber. Under these conditions, tip size is expected to limit spatial resolution, providing much better resolution than in the case of embedded objects. Spectromicroscopy resolution values of approximately 50 nm in spectromicroscopy and 25 nm in imaging have been reported when measuring supported monomolecular layers on gold, comparable to tip size.[30]

The images in the Supporting Information Figure S3 have been collected using both H polarization and V polarization. Surface selectivity improves at the higher frequency for both polarizations, indicating that effects due to optical enhancement at the tip are minor or absent, while photothermal properties dominate the response of the system. Enhancement due to the optics of the tip is expected to provide a much stronger signal when measuring with V polarization, roughly parallel to the axis of the tip. In addition, depth response would also be dominated by the extension of the enhanced electric field at the tip, which is of the order of tens of nanometers. Neither of the latter effects

https://dx.doi.org/10.1021/acs.analchem.9b03468
Anal. Chem. 2020, 92, 3544−3554

are observed. Therefore, we conclude that we do not observe strong effects of optical enhancement in our experiments, either on resolution or on signal intensity. The conclusion is also consistent with the relatively large diameter of our tip (Supporting Information Section S7), which is not optimized for surface enhancement effects.

CONCLUSIONS

We have performed a systematic study of the effect of laser pulse structure on resonant PTIR signal generation and spatial resolution. Experimental results are only partially described by existing theoretical treatments of PTIR resolution and of PTIR signal generation. Measured resolution values are intermediate between the thermal diffusion limit and conventional AFM resolution. Higher frequency, longer pulses, and a shorter interval between pulses improve resolution in the sample plane by decreasing the width of the photothermal expansion region at the boundary of an absorbing material. Therefore, in-plane resolution depends on the interplay of sample expansion and tip size. Its value is larger than tip radius, but becomes comparable to, and even smaller than, tip radius for the highest frequency and longest pulse duration available from the instrument in use.

We note some small differences in the resolution values of spectromicroscopy experiments and imaging experiments, with the latter providing poorer resolution. The reason for this discrepancy is presently unclear and may arise from the interplay of tip movement, instrumental parameters, and the mechanism of PTIR signal generation.

We show that spatial resolution does not depend linearly on the temperature increase in the sample and is not adequately described by the familiar distribution of a thermal wave through the sample or any of the parameters derived from it, such as R and L, in contrast with other photothermal techniques. The present experiments do not quantitatively assess resolution and depth response in the direction perpendicular to the sample surface. Nonetheless, we can appreciate that the depth response is also better than expected from thermal wave distribution.

We show that the intensity of the PTIR signal also depends on the structure of the pulse train, similarly to resolution. It increases with a longer pulse length and shorter interval between pulses. Based on this observation, we conclude that resonant PTIR intensity is determined by the nonlinearity of sample excitation as a function of temperature. This interpretation also explains the dependence of resonant PTIR spatial resolution from the pulse structure used for excitation. Experiments of microphotoacoustic spectroscopy (micro-PAS)[31] at variable excitation frequency will be carried out to confirm or refute this hypothesis. By analogy with super-resolved optical microscopy, we propose that the nonlinear response of the sample is the factor that allows resonant PTIR to overcome the resolution limits set by thermal waves. In this sense, resonant PTIR can be considered a technique for super-resolved photothermal microscopy and spectroscopy.

We do not presently have quantitative information to assess the limiting depth response of the PTIR measurement, but it appears to be affected by pulse structure similarly to in-plane resolution. In addition, the detail observed from the imaging of the PMMA surface in Figure 3, though still unexplained, suggests that surface sensitivity and selectivity also depend on the nature of the tip−sample contact at the molecular level. The sensitivity of resonant PTIR to monomolecular layers was previously demonstrated using optical tip enhancement. Here, we show that high sensitivity, surface selectivity, and spatial resolution can be achieved without tip enhancement, by controlling the photothermal expansion process.

It is notable that the minimum achievable resolution in spectromicroscopy measurements can be smaller than tip radius. In the present measurements, limits set by the instrumentation do not allow us to explore smaller resolution values. However, the resolution values demonstrated in this work are already approaching the size of larger individual macromolecules. We suggest that by extending the accessible pulse frequency values, smaller proteins and single small molecules may be eventually accessible.

In conclusion, we achieved a new level of understanding and control of the parameters that govern resolution and depth profiling in resonant PTIR, which opens the way to the controlled analysis of complex samples, such as layered samples or samples with a core−shell structure. This includes many samples of interest for technological applications and for the material, environmental, biomedical, and biological sciences.

ASSOCIATED CONTENT

Supporting Information

The Supporting Information is available free of charge at https://pubs.acs.org/doi/10.1021/acs.analchem.9b03468.

Notes on in-plane resolution of PTIR measurements, thermal wavelength and thermal wave distribution, sample image profiles, direct temperature measurements of PMMA bead sections, effect of light polarization, definition of the Grüneisen parameter, dimensions of PTIR tips, and resolution and thermal wavelength equations, and figures of PTIR imaging line profiles, STIRM spectra and STIRM images of PMMA, calculations of surface temperature distribution, SEM images of tip (PDF)

AUTHOR INFORMATION

Corresponding Author

Luca Quaroni − *Department of Physical Chemistry and Electrochemistry, Faculty of Chemistry, Jagiellonian University 30-387 Kraków, Poland;* orcid.org/0000-0002-0225-9775; Email: luca.quaroni@uj.edu.pl

Complete contact information is available at: https://pubs.acs.org/10.1021/acs.analchem.9b03468

Notes

The author declares no competing financial interest.

ACKNOWLEDGMENTS

The research was performed using equipment purchased in the frame of the project cofunded by the Małopolska Regional Operational Programme Measure 5.1 Krakow Metropolitan Area as an important hub of the European Research Area for 2007−2013, project no. MRPO.05.01.00-12-013/15. During this work, L.Q. was supported by the European Union's Horizon 2020 research and innovation programme under the Marie Skłodowska-Curie grant agreement no. 665778, managed by the National Science Center Poland under POLONEZ contract 2016/21/P/ST4/01321, and by an OPUS16 grant from the National Science Center Poland under contract 2018/31/B/NZ1/01345. The author is grateful to his spouse, Theodora Zlateva, for supporting him financially throughout part of this work. The author is particularly grateful to Dr. Kirk Michaelian, Natural Resources Canada, for discussions over photothermal

spectroscopy and for critically reading the manuscript. Helpful discussions with Dr. Gianfelice Cinque and Dr. Mark Frogley, Diamond Light Source, are also gratefully acknowledged. The author thanks prof. dr. hab. Czesława Paluszkiewicz, prof. dr. hab. Wojciech Kwiatek, dr. Natalia Piergies, and dr. Ewa Pięta of IFJ-PAN for nanoIR2 instrumentation access, support, and advice, and dr. Michał Pacia and the Team of Photocatalysis of Jagiellonian University for the SEM measurements. The author also acknowledges Dr. Kingshuk Bandopadhyay of Jagiellonian University for reading the manuscript and for helpful comments and prof. dr. hab. Maria Nowakowska for reading the manuscript and for the support through the Polonez project. Thanks are also given to Dr. Miriam Unger, Dr. Anirban Roy, and the staff of Anasys/Bruker for information and discussion about the instrumentation. The author is grateful to the reviewer who helped improving the manuscript with extremely challenging and pertinent criticism.

REFERENCES

(1) Centrone, A. *Annu. Rev. Anal. Chem.* **2015**, *8* (1), 101−126.
(2) Dazzi, A.; Prazeres, R.; Glotin, F.; Ortega, J. M. *Opt. Lett.* **2005**, *30* (18), 2388.
(3) Morris, M. D.; Peck, K. *Anal. Chem.* **1986**, *58* (7), 811A−822A.
(4) Hammiche, A.; Pollock, H. M.; Reading, M.; Claybourn, M.; Turner, P. H.; Jewkes, K. *Appl. Spectrosc.* **1999**, *53* (7), 810−815.
(5) Katzenmeyer, A. M.; Holland, G.; Chae, J.; Band, A.; Kjoller, K.; Centrone, A. *Nanoscale* **2015**, *7* (42), 17637−17641.
(6) Rosencwaig, A.; Gersho, A. *J. Appl. Phys.* **1976**, *47* (1), 64−69.
(7) Jackson, W. B.; Amer, N. M.; Boccara, A. C.; Fournier, D. *Appl. Opt.* **1981**, *20* (8), 1333.
(8) Dazzi, A. PhotoThermal Induced Resonance. Application to Infrared Spectromicroscopy. In *Thermal Nanosystems and Nanomaterials*; Volz, S., Ed.; Springer: Berlin, Germany, 2009; pp 469−503.
(9) Donaldson, P. M.; Kelley, C. S.; Frogley, M. D.; Filik, J.; Wehbe, K.; Cinque, G. *Opt. Express* **2016**, *24* (3), 1852.
(10) Rosencwaig, A. *Science (Washington, DC, U. S.)* **1982**, *218* (4569), 223−228.
(11) Morozovska, A. N.; Eliseev, E. A.; Borodinov, N.; Ovchinnikova, O. S.; Morozovsky, N. V.; Kalinin, S. V. *Appl. Phys. Lett.* **2018**, *112* (3), 1−16.
(12) Dazzi, A.; Prater, C. B. *Chem. Rev.* **2017**, *117* (7), 5146−5173.
(13) Levenson, E.; Lerch, P.; Martin, M. C. *Infrared Phys. Technol.* **2006**, *49* (1−2), 45−52.
(14) Lu, F.; Belkin, M. A. *Opt. Express* **2011**, *19* (21), 19942−19947.
(15) Hammiche, A.; Bozec, L.; Pollock, H. M.; German, M.; Reading, M. *J. Microsc.* **2004**, *213* (2), 129−134.
(16) Donaldson, P. M.; Kelley, C. S.; Frogley, M. D.; Filik, J.; Wehbe, K.; Cinque, G. *Opt. Express* **2016**, *24* (3), 1852.
(17) Bozec, L.; Hammiche, A.; Pollock, H. M.; Conroy, M.; Chalmers, J. M.; Everall, N. J.; Turin, L. *J. Appl. Phys.* **2001**, *90* (10), 5159−5165.
(18) Michaelian, K. H. *Photoacoustic Infrared Spectroscopy*; John Wiley & Sons: Hoboken, NJ, 2003.
(19) Opsal, J.; Rosencwaig, A. *J. Appl. Phys.* **1982**, *53* (6), 4240.
(20) Mandelis, A.; Salnick, A.; Opsal, J.; Rosencwaig, A. *J. Appl. Phys.* **1999**, *85* (3), 1811−1821.
(21) Zharov, V. P.; Letokhov, V. S. *Laser Optoacoustic Spectroscopy*; Springer: Berlin, Germany, 1986.
(22) Chae, J.; An, S.; Ramer, G.; Stavila, V.; Holland, G.; Yoon, Y.; Talin, A. A.; Allendorf, M.; Aksyuk, V. A.; Centrone, A. *Nano Lett.* **2017**, *17* (9), 5587−5594.
(23) Mathurin, J.; Pancani, E.; Deniset-Besseau, A.; Kjoller, K.; Prater, C. B.; Gref, R.; Dazzi, A. *Analyst* **2018**, *143* (24), 5940−5949.
(24) Dazzi, A.; Glotin, F.; Carminati, R. *J. Appl. Phys.* **2010**, *107* (12), 124519.
(25) Katzenmeyer, A. M.; Aksyuk, V.; Centrone, A. *Anal. Chem.* **2013**, *85* (4), 1972−1979.
(26) Wang, L.; Zhang, C.; Wang, L. V. *Phys. Rev. Lett.* **2014**, *113* (17), 1−5.
(27) Quaroni, L.; Pogoda, K.; Wiltowska-Zuber, J.; Kwiatek, W. M. *RSC Adv.* **2018**, *8* (5), 2786−2794.
(28) Paluszkiewicz, C.; Piergies, N.; Chaniecki, P.; Rękas, M.; Miszczyk, J.; Kwiatek, W. M. *J. Pharm. Biomed. Anal.* **2017**, *139*, 125−132.
(29) Quaroni, L. *Molecules* **2019**, *24* (24), 4504.
(30) Lu, F.; Jin, M.; Belkin, M. A. *Nat. Photonics* **2014**, *8* (4), 307−312.
(31) Michaelian, K. H.; Frogley, M. D.; Kelley, C. S.; Pedersen, T.; May, T. E.; Quaroni, L.; Cinque, G. *Infrared Phys. Technol.* **2018**, *93*, 240−246.

https://dx.doi.org/10.1021/acs.analchem.9b03468
Anal. Chem. 2020, 92, 3544−3554